Planta (2016) 243:1143–1158
DOI 10.1007/s00425-016-2470-1

ORIGINAL ARTICLE

Lignin–carbohydrate complexes from sisal (*Agave sisalana*) and abaca (*Musa textilis*): chemical composition and structural modifications during the isolation process

José C. del Río[1] · Pepijn Prinsen[1] · Edith M. Cadena[1] · Ángel T. Martínez[2] · Ana Gutiérrez[1] · Jorge Rencoret[1]

Received: 19 October 2015 / Accepted: 14 January 2016 / Published online: 5 February 2016

Abstract

Main conclusion **Two types of lignins occurred in different lignin–carbohydrate fractions, a lignin enriched in syringyl units, less condensed, preferentially associated with xylans, and a lignin with more guaiacyl units, more condensed, associated with glucans.**

Lignin–carbohydrate complexes (LCC) were isolated from the fibers of sisal (*Agave sisalana*) and abaca (*Musa textilis*) according to a plant biomass fractionation procedure recently developed and which was termed as "universally" applicable to any type of lignocellulosic material. Two LCC fractions, namely glucan–lignin (GL) and xylan–lignin (XL), were isolated and differed in the content and composition of carbohydrates and lignin. In both cases, GL fractions were enriched in glucans and comparatively depleted in lignin, whereas XL fractions were depleted in glucans, but enriched in xylans and lignin. Analysis by two-dimensional Nuclear Magnetic Resonance (2D-NMR) and Derivatization Followed by Reductive Cleavage (DFRC) indicated that the XL fractions were enriched in syringyl (S)-lignin units and β-*O*-4′ alkyl-aryl ether linkages, whereas GL fractions have more guaiacyl (G)-lignin units and less β-*O*-4′ alkyl-aryl ether linkages per lignin unit. The data suggest that the structural characteristics of the lignin polymers are not homogeneously distributed within the same plant and that two different lignin polymers with different composition and structure might be present. The analyses also suggested that acetates from hemicelluloses and the acyl groups (acetates and *p*-coumarates) attached to the γ-OH of the lignin side chains were extensively hydrolyzed and removed during the LCC fractionation process. Therefore, caution must be paid when using this fractionation approach for the structural characterization of plants with acylated hemicelluloses and lignins. Finally, several chemical linkages (phenylglycosides and benzyl ethers) could be observed to occur between lignin and xylans in these plants.

Keywords Glucan–lignin · Xylan–lignin · Acetates · *p*-Coumarates · Lignin–carbohydrate linkages

Introduction

Lignin, cellulose and hemicelluloses are the three major structural components of plant cell walls. However, selective separation or fractionation of these components is difficult because they are physically entangled among them in the cell wall (Fengel and Wegener 1984). In addition, chemical linkages can also occur between these components, forming the so-called lignin–carbohydrate complexes (LCCs) (Fengel and Wegener 1984; Koshijima and Watanabe 2003; Balakshin et al. 2011). The linkage types are still not well understood, although it is generally accepted that there are three types of lignin–carbohydrate linkages present in wood, namely phenyl glycosides, esters, and benzyl ethers (Fengel and Wegener 1984). The tight physical binding and chemical linkages between lignin and cell wall carbohydrates prevents the isolation of the different components in an unaltered manner. Our knowledge about the LCCs is still limited and additional investigations are needed to provide information regarding the bonding

✉ José C. del Río
delrio@irnase.csic.es

[1] Instituto de Recursos Naturales y Agrobiología de Sevilla, CSIC, P.O. Box 1052, 41080 Seville, Spain

[2] Centro de Investigaciones Biológicas, CSIC, Ramiro de Maeztu 9, 28040 Madrid, Spain

relationships among cellulose, hemicelluloses and lignin. However, and to investigate the structure of LCC, a clear and complete fractionation with proper preservation of the bonds between the lignin and carbohydrates must be obtained. In addition, for detailed structural investigations, isolation of LCCs in chemically unaltered forms is a prerequisite.

An earlier attempt to quantitatively fractionate plant cell wall components was based on ball milling, followed by endoglucanase enzymatic hydrolysis and alkaline dissolution, an approach by which all of the lignin in softwood was isolated as various LCCs (Lawoko et al. 2003, 2005). A major limitation of this method, however, is that it involved many steps and is only applicable to softwoods, which strongly restricts its application. More recently, another much simpler fractionation method was established to isolate LCCs from lignocellulosic biomass based on mild milling (for structural preservation) and dissolution using a mixture of dimethyl sulfoxide (DMSO) and 50 % (v/v) aqueous tetrabutylammonium hydroxide (TBAH) (Li et al. 2011; Du et al. 2013, 2014). This method successfully provides clear and complete fractionation of LCCs from hardwoods, e.g., eucalyptus (Li et al. 2011), and softwoods, e.g., spruce (Du et al. 2013, 2014). Two LCC fractions, a glucan–lignin (GL) and a xylan–lignin (XL) fraction, were quantitatively obtained from hardwoods, while a glucomannan–lignin (GML) fraction was additionally obtained from softwoods by using this fractionation approach. Because the method quantitatively fractionates all types of lignocellulosic biomass, including hardwoods (Li et al. 2011), softwoods (Du et al. 2013, 2014) as well as non-woody chemical pulps (Cadena et al. 2011), the fractionation approach was alleged to be 'universally' applicable to any type of wood, pulp and any other processed lignocellulosic biomass. Moreover, it was also claimed that the method isolates all cell wall components, including carbohydrates and lignin, in a chemically unaltered form, which is of high importance for subsequent structural studies.

However, it is questionable whether this method can efficiently recover all plant cell wall components without any structural modification given that it uses TBAH, a strong base that may alter the structure of the carbohydrates and lignin by causing hydrolysis of the acyl groups attached to these polymers and thus hindering its potential use for subsequent structural studies. The hemicelluloses and the lignin in the plant cell walls are known to be partially acetylated. Glucomannans are the major constituents of softwood hemicelluloses, which are usually acetylated at the C-2 and/or C-3 positions of the mannosyl unit (Willför et al. 2003). In hardwoods, the predominant hemicellulose is xylan that consists of D-xylopyranose units in the backbone linked by β-(1 → 4) glycosidic bonds. Around 70 % of the D-xylopyranose residues in hardwoods are acetylated at the C-2 and/or C-3 positions (Teleman et al. 2002; Sjöström 1993). Hemicelluloses in annual plants can also be acetylated, and an acetylated heteroxylan has recently been described in sisal with around 60 % of the D-xylopyranose units being acetylated (Marques et al. 2010). On the other hand, the lignins of many plants are also known to be partially acylated (with acetates, *p*-coumarates and *p*-hydroxybenzoates) at the γ-OH of the lignin side chain, and predominantly on syringyl units (Landucci et al. 1992; Ralph 1996, 2010; Lu and Ralph 1999, 2005; Ralph et al. 1994, 2004; Ralph and Lu 1998; del Río et al. 2004, 2007, 2008, 2012a, b, 2015; Rencoret et al. 2013; Lu et al. 2015). In particular, acetylated lignin units are known to widely occur—and are probably ubiquitous—in all angiosperms, including mono- and eudicotyledons (del Río et al. 2007). In some plants, such as sisal and abaca, lignin acylation occurs to a very high extent, reaching up to 80 % of the uncondensed syringyl lignin units (del Río et al. 2007, 2008; Martínez et al. 2008). The occurrence of acetates, *p*-coumarates or *p*-hydroxybenzoates, naturally occurring on lignin, has traditionally been biased due to the limitations of the analytical procedures used for their isolation and/or structural characterization, and these acyl groups have been hydrolyzed and removed when using traditional isolation methods (such as alkaline extraction often applied to non-woody lignins). Therefore, it can be envisaged that the use of TBAH, a strong basic reagent, to separate the LCC fractions according to the protocol recently described could also affect to a large extent the acetates in hemicelluloses and the acyl groups attached to the γ-OH in lignin impeding to obtain accurate structural information of these structural polymers.

In this paper, we have applied the LCC fractionation approach recently developed (Li et al. 2011; Du et al. 2013, 2014) to sisal (*Agave sisalana*) and abaca (*Musa textilis*), two plants that are known to contain acetylated carbohydrates and that also have lignins with a high extent of acylation of the γ-OH. The composition and structure of the isolated LCC fractions were studied by 2D NMR, which provided useful information regarding the structure of these fractions as well as the eventual structural changes occurring during the LCC isolation process. In addition, the fate of acetate groups attached to the lignin units was also monitored by using a modification of the so-called Derivatization Followed by Reductive Cleavage (DFRC) method (Lu and Ralph 1997a, b, 1998). DFRC is a degradation method that selectively cleaves β-*O*-4′ alkyl-aryl ether linkages but leaves γ-esters intact. The original DFRC method uses acetylating reagents that interfere in the analysis of native acetates in lignin, but with appropriate modification by substituting acetylation by propionylation (Ralph and Lu 1998), it is possible to obtain

significant information about the extent of native lignin acetylation. Finally, the possible linkages occurring among the carbohydrates and lignin will also be studied. This study will provide important information to better understand the chemical structure and relationships between the structural components of the plant cell walls.

Materials and methods

Plant samples

The plant samples selected for this study consisted of leaf fibers of sisal (*A. sisalana*) and abaca (*M. textilis*) that were provided by CELESA pulp mill (Tortosa, Spain). The fibers were air-dried and finely ground to sawdust using a knife mill (IKA-Werke MF10, Staufen, Germany) and passing through a 1 mm mesh size before the analysis. The water-soluble and lipophilic extractives were removed using hot water (3 h—100 °C) followed by Soxhlet extraction with acetone to obtain extractive-free samples.

Lignin–carbohydrate complex (LCC) from biomass

The LCC fractionation was performed according to the method previously described (Li et al. 2011; Du et al. 2013) and detailed in the flowchart of Fig. 1. Around 3 g of plant samples were ball-milled in a PM100 planetary ball mill (Restch, Haan, Germany) at 400 rpm in an agate jar and using agate balls (20 × 20 mm). The total ball-milling time was 6 h, with 10 min breaks after every 10 min of milling. The ball-milled sample was completely dissolved in a mixture of 30 mL dimethylsulfoxide (DMSO) under stirring followed by the addition of 30 mL tetrabutylammonium hydroxide (TBAH; 40 % w/w in water). After complete dissolution, it was dispersed into 500 mL deionized water under stirring until a precipitate was formed. The precipitate was centrifuged and washed with deionized water until neutral pH, and was then freeze-dried to obtain the glucan–lignin fraction (GL). The xylan–lignin fraction (XL) was obtained after separation of the precipitate, by neutralizing the solution with HCl, followed by dialysis (Spectra/Por Dialysis Tubing MWCO 1000 D) and freeze-drying. The barium hydroxide step detailed in Du et al. (2013) was skipped since glucomannan is not a major hemicellulose in these plants, as also occurs in hardwoods (Li et al. 2011).

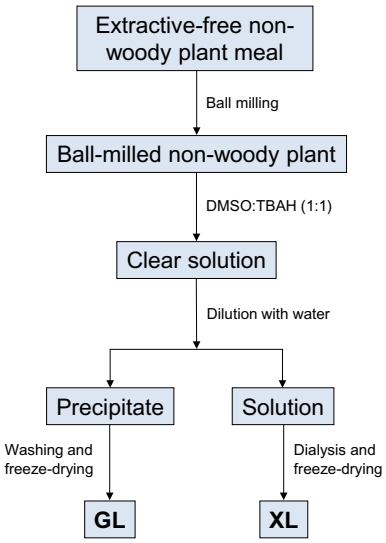

Fig. 1 Flowchart of the LCC fractionation approach used in this study (*GL* glucan–lignin, *XL* xylan–lignin). Adapted from Li et al. (2011) and Du et al. (2013)

Determination of the Klason lignin content and sugar composition

The Klason lignin content was determined as the residue after sulfuric acid hydrolysis of the material according to the TAPPI method T222 om-88 (Tappi 2004). The lignin content was then corrected for ash and protein, as determined from the mass fraction of atomic nitrogen obtained by CHN elemental analysis in a LECO CHNS-932 Elemental Analyzer (LECO Corp., St. Joseph, Mich.) and using a 6.25 conversion factor (Darwill et al. 1980). The composition and content of neutral sugars in the hydrolysates were analyzed, after neutralization with barium carbonate, by high-performance liquid (HPLC) using an Agilent 1200 series HPLC system (Agilent Technologies, USA) equipped with a refractive index detector (RID); the analytical ion exchange column Aminex HPX-87H was used and protected with a guard cartridge (Bio-Rad, USA). The analyses by HPLC were performed at 60 °C under isocratic conditions; the mobile phase consisted of H_2SO_4 6 mM, flow rate of 0.6 mL/min and injection volume of 20 µL. Carbohydrate composition (arabinose, xylose, mannose, galactose, glucose) was analyzed by interpolation into calibration curves run from standards. Two replicates were used for each sample.

'Milled-wood' lignin (MWL) isolation

'Milled-wood' lignins (MWLs) were extracted according to the classical procedure (Björkman 1956). Around 50 g of extractive-free sisal and abaca was finely ball-milled in a Retsch PM100 planetary ball mill (Restch, Haan, Germany) at 400 ppm (35 h) using an agate jar and 20 agate balls of 2 cm diameter (this finely ball-milled material was used directly for whole cell wall-NMR to determine compositional and structural features). The ball-milled material was then extracted with dioxane–water (9:1, v/v), followed

by evaporation of the solvent, and purified as described elsewhere (del Río et al. 2012b). The final yields ranged from 5 to 15 % of the original lignin content. Extension of milling time, which would increase yield, was avoided to prevent chemical modifications on the lignin structure.

Nuclear magnetic resonance (NMR) spectroscopy

For NMR analysis of the whole cell walls and the isolated LCC fractions, around 50 mg of finely divided (ball-milled, 35 h) samples was swollen in 0.75 mL DMSO-d_6 according to the method previously described (Kim et al. 2008; Rencoret et al. 2009). Under these conditions the cellulose is undetectable in the NMR spectra due to its reduced mobility. To make the cellulose visible in the spectra, the LCCs fractions were also acetylated in DMSO/*N*-methylimidazole/acetic anhydride, according to the method described in Mansfield et al. (2012), and dissolved in 0.75 mL of $CDCl_3$ for additional NMR analysis. In the case of the isolated MWLs, around 40 mg of sample was dissolved in 0.75 mL of DMSO-d_6. NMR spectra were recorded at 25 °C on an AVANCE III 500 MHz instrument (Bruker, Karlsruhe, Germany) equipped with a cryogenically cooled z-gradient triple-resonance probe at the NMR facilities of the General Research Services of the University of Seville. HSQC (heteronuclear single-quantum correlation) experiments used Bruker's 'hsqcetgpsisp2.2′ adiabatic pulse program with spectral widths of 5000 Hz (from 10 to 0 ppm) and 20,625 Hz (from 165 to 0 ppm) for the ^{1}H- and ^{13}C-dimensions. The number of collected complex points was 2048 for the ^{1}H-dimension with a recycle delay of 1 s. The number of transients was 64, and 256 time increments were recorded in ^{13}C-dimension. The $^{1}J_{CH}$ used was 140 Hz. Processing used typically matched Gaussian apodization in ^{1}H (LB = −0.1, GB = 0.001) and a squared cosine-bell and one level linear prediction (32 coefficients) in ^{13}C. Prior to Fourier transformation, the data matrices were zero-filled up to 1024 points in the ^{13}C-dimension. Phase correction was manually applied to the total spectrum, while the baseline was automatically corrected in both dimensions. The central solvent peaks were used as internal references (δ_C/δ_H 39.5/2.49 for DMSO and 70.0/7.26 for $CHCl_3$). HSQC cross-signals were assigned by comparison with the literature (Martínez et al. 2008; Kim et al. 2008; Rencoret et al. 2009; Ralph et al. 2009; del Río et al. 2008, 2012a). A semiquantitative analysis of the volume integrals of the HSQC signals was performed using the Bruker's Topspin 3.1 processing software and by turning off the linear prediction. In the aliphatic oxygenated region, the relative abundances of side chains involved in inter-unit linkages or present in terminal units were estimated from the C_α/H_α correlations to avoid possible interference from homonuclear ^{1}H–^{1}H couplings. In the aromatic/unsaturated region of the spectra, C_2/H_2 correlations from H-, G- and S-lignin units and from *p*-coumarates were used to estimate their relative abundances. By using the above adiabatic pulse it was possible to refer to the abundances of the different interunit linkages, as well as the *p*-coumarate content, to the number of aromatic units (as per 100 aromatic units; H + G + S = 100) calculated from their respective volume integrals.

DFRC (derivatization followed by reductive cleavage) degradation

A modification of the standard DFRC method by using propionyl instead of acetyl reagents (DFRC′) was used (Ralph and Lu 1998). Lignins (10 mg) were stirred for 2 h at 50 °C with propionyl bromide in propionic acid (8:92, v/v). The solvents and excess of bromide were removed by rotary evaporation. The products were then dissolved in dioxane/propionic acid/water (5:4:1, v/v/v) and 50 mg powered Zn was added. After 40 min stirring at room temperature, the mixture was transferred into a separatory funnel with dichloromethane and saturated ammonium chloride. The aqueous phase was adjusted to pH < 3 by adding 3 % HCl, the mixture vigorously mixed, and the organic layer separated. The water phase was extracted twice more with dichloromethane. The combined dichloromethane fractions were dried over anhydrous Na_2SO_4 and the filtrate was evaporated in a rotary evaporator. The residue was subsequently propionylated for 1 h in 1.1 mL of dichloromethane containing 0.2 mL of propionic anhydride and 0.2 mL pyridine. The propionylated lignin degradation compounds were collected after rotary evaporation of the solvents and subsequently analyzed by GC/MS.

The GC/MS analyses were performed with a Varian model Star 3800 GC equipped with an Ion Trap detector (Varian model Saturn 4000) using a 15 m capillary column (DB-5HT, 5 m × 0.25 mm I.D., 0.1 μm film thickness) from J&W Scientific. The oven was heated from 120 (1 min) to 330 °C at 6 °C/min and held for 4 min at the final temperature. The injector was programmed from 60 to 350 °C at a rate of 200 °C/min and held until the end of the analysis. The transfer line was kept at 300 °C. Helium was used as the carrier gas at a rate of 2 mL/min.

Results and discussion

Isolation and composition of LCC fractions from sisal and abaca

Sisal and abaca fibers were fractionated according to the LCC fractionation approach previously developed (Li et al.

Table 1 Yields of GL and XL fractions isolated from sisal and abaca, and content of Klason lignin and carbohydrates in the whole cell walls (CW) and their isolated fractions

	Sisal			Abaca		
	CW	GL	XL	CW	GL	XL
Yield (%)	–	64.7	29.3	–	74.4	19.4
Klason lignin (%)	8.5	7.8	24.1	9.3	4.4	29.4
Carbohydrates (relative %)						
Arabinose	0.4	1.5	0.6	1.2	0.3	3.4
Xylose	18.3	9.0	89.4	8.6	4.1	75.5
Mannose	0.5	0.9	2.6	3.0	0.5	13.0
Galactose	0.2	0.2	0.3	0.2	0.1	0.3
Glucose	80.6	88.4	7.1	87.0	95.0	7.8

2011; Du et al. 2013), and detailed in Fig. 1. Two different LCC fractions, namely a glucan–lignin (GL) and a xylan–lignin (XL) fraction, were efficiently and quantitatively isolated. The yields of the GL and XL fractions, as well as the Klason lignin content and the composition of the sugars in these fractions, are detailed in Table 1. The GL and XL fractions isolated from sisal accounted for 64.7 and 29.3 %, respectively, whereas the GL and XL fractions isolated from abaca accounted for 74.4 and 19.4 %, respectively. In both plants, the yields of GL were higher than XL, as also occurred in hardwoods and softwoods (Li et al. 2011; Du et al. 2013). In addition, the analysis of the Klason lignin content and sugar composition indicates that, in both plants, the GL fractions were enriched in glucans (88.4 and 95.0 % of glucose in sisal and abaca) and depleted in lignin (7.8 and 4.4 % Klason lignin content in sisal and abaca), while the XL fractions were enriched in xylans (89.4 and 75.5 % of xylose in sisal and abaca) and lignin (24.1 and 29.4 % Klason lignin content in sisal and abaca) and depleted in glucans. Similar results were also observed in the LCC fractions isolated from hardwoods and softwoods by using this fractionation procedure (Li et al. 2011; Du et al. 2013, 2014) and indicate an association between lignin and xylans in these plants.

Structure and composition of the LCC fractions as seen by 2D HSQC NMR

The GL and XL fractions isolated from sisal and abaca were analyzed by 2D HSQC NMR and their spectra were compared with those of their respective whole cell walls and isolated MWLs (Figs. 2, 3). The main lignin and carbohydrate signals assigned in the HSQC spectra are listed in Table 2 and the main substructures present are depicted in Fig. 4.

The HSQC spectra of the whole cell walls of sisal and abaca show strong signals from carbohydrates and lignin, whereas the spectra from the MWLs essentially show a predominance of lignin signals. The most important carbohydrate signals corresponded to C_2/H_2, C_3/H_3, C_4/H_4, and C_5/H_5 correlations of xylans (**X_2**, **X_3**, **X_4**, **X_5**) and the C_4/H_4 correlation for 4-*O*-methyl-α-D-glucuronic acid (**U_4**), which is more evident in sisal. Signals from *O*-acetylated xylans (3-*O*-acetyl-β-D-xylopyranoside, **X'_3**, and 2-*O*-acetyl-β-D-xylopyranoside, **X'_2**) were also clearly evident in the spectra of whole cell walls of sisal and abaca, confirming that xylans are partially acetylated at C-2 and/or C-3. Other carbohydrate signals included the C_1/H_1 correlations for the anomeric carbons of β-D-xylopyranoside (**X_1**), 2-*O*-acetyl-β-D-xylopyranoside (**X'_1**), β-D-glucopyranoside (**Gl_1**), and 4-*O*-methyl-α-D-glucuronic acid (**U_1**). Lignin signals were also observed in the HSQC spectra of the whole cell walls, although they were more clear in the spectra of the isolated MWLs. Lignin signals included the C_α/H_α, C_β/H_β and C_γ/H_γ correlations from the different lignin inter-unit linkages, including β-*O*-4′ alkyl-aryl ether linkages (**A**, **A′**), phenylcoumarans (**B**), resinols (**C**), spirodienones (**E**) and cinnamyl alcohol end groups (**I**, **I′**), among others, as well as signals for *p*-hydroxyphenyl (**H**), guaiacyl (**G**), and syringyl (**S**) lignin aromatic units, and signals from *p*-coumarates (**PCA**) in the case of abaca lignin. The spectra of the whole cell walls and their corresponding MWLs also showed the occurrence of intense signals in the range δ_C/δ_H 62.7/3.83–4.30 assigned to the C_γ/H_γ correlations of γ-acylated lignin units (**A′**), revealing that these lignins are extensively acylated at the γ-OH of the lignin side chain, as previously observed (del Río et al. 2007, 2008; Martínez et al. 2008). The lignin from sisal is known to be acylated exclusively with acetate groups, whereas the lignin from abaca is acylated with both acetate and *p*-coumarate groups (del Río et al. 2007, 2008; Martínez et al. 2008). An estimation of the extent of γ-acylation of the lignin side chains was performed by integration of the signals corresponding to the C_γ/H_γ correlations of γ-OH versus the γ-acylated units in the HSQC spectra of the isolated MWLs (where the signals from carbohydrates do not interfere) and amounted to 65 % in sisal and to 80 % in abaca. The spectra also showed other signals from γ-acylated lignin units. The C_α/H_α correlations in normal (γ-OH) and γ-acylated β-*O*-4′ substructures (**A**, **A′**) were observed at δ_C/δ_H 71.8/4.87, whereas the C_β/H_β correlations were observed at δ_C/δ_H 85.9/4.12 in normal (γ-OH) β-*O*-4′ substructures linked to an S unit but shifted to δ_C/δ_H 83.0/4.33 in γ-acylated β-*O*-4′ substructures (**A′**), which overlaps with the C_β/H_β correlations of normal (γ-OH) β-*O*-4′ substructures linked to a G unit at δ_C/δ_H 83.6/4.29. The C_β/H_β correlations of γ-acylated β-*O*-4′ substructures linked to G units shifted to δ_C/δ_H 80.8/4.58 and were clearly visible in the HSQC spectrum of the MWL from sisal, indicating an important γ-acylation extent of G-lignin units in this

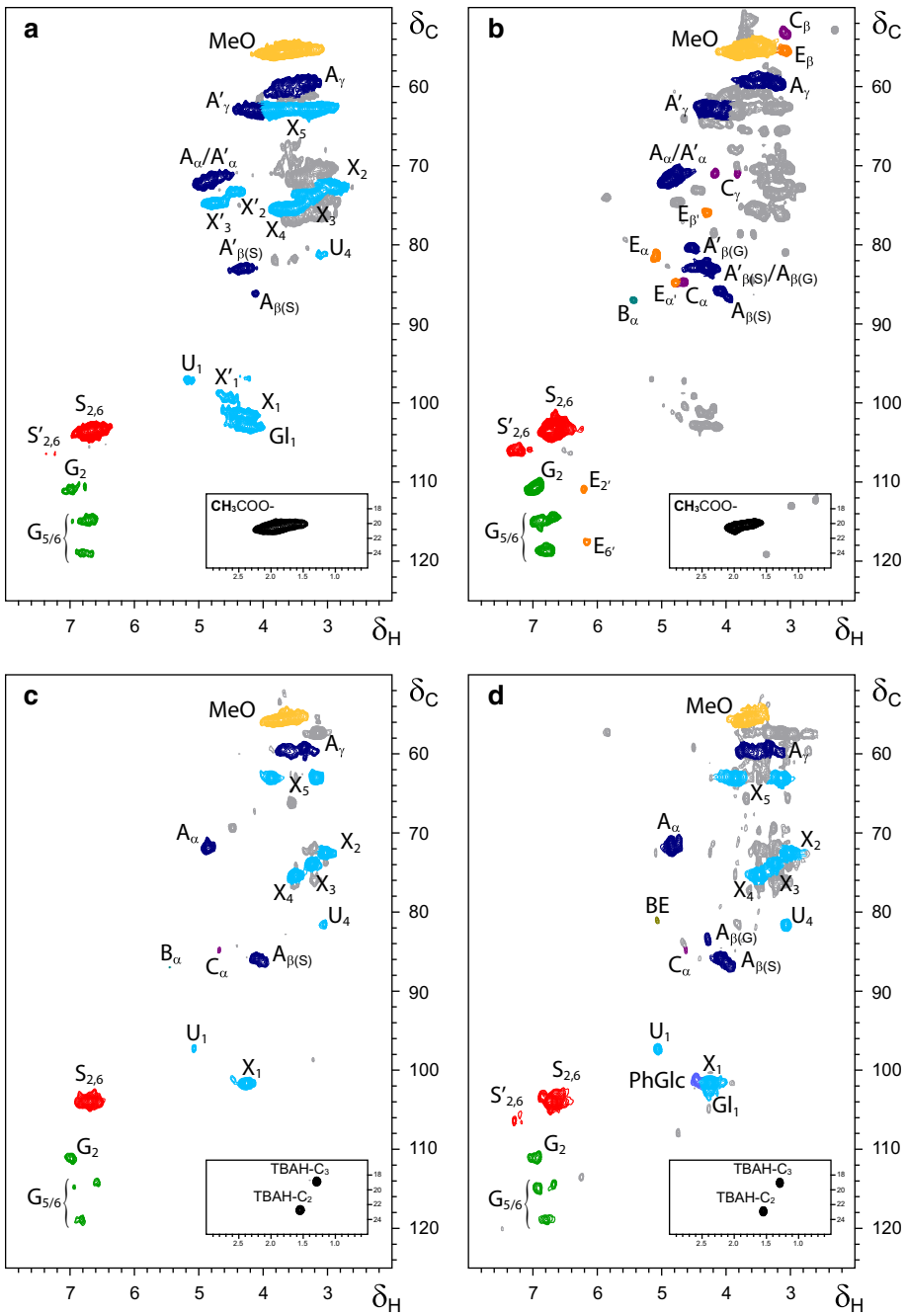

Fig. 2 2D HSQC NMR spectra (δ_C/δ_H 50–125/2.0–8.0) of **a** whole cell walls from sisal, **b** MWL isolated from sisal, **c** GL fraction from sisal, and **d** XL fraction from sisal. See Table 2 for signal assignments and Fig. 4 for the main lignin structures identified

particular lignin, which was minor in the HSQC of the MWL from abaca. Finally, the insets of Figs. 2 and 3 also show the signal at δ_C/δ_H 20–21/1.50–2.00 from acetate groups attached to the lignin (and also to hemicelluloses in the case of the whole cell walls). On the other hand, the HSQC of the abaca MWL showed the absence of β–β′ resinols (**C**), but instead presented a β–β′-tetrahydrofuran structure (**C′**) that arises from β–β′ coupling of two sinapyl *p*-coumarates (Lu and Ralph 2005; Martínez et al. 2008; del Río et al. 2012b) and that reflects the high extent of γ-acylation of abaca lignin with *p*-coumarates.

Most of the carbohydrate and lignin signals observed in the spectra of the whole cell walls and the MWLs were also present in the spectra of the GL and XL fractions. The HSQC spectra of the GL fractions showed mostly signals from carbohydrates, whereas lignin signals were observed at low intensities in accordance with their low lignin contents (7.8 and 4.4 % Klason lignin content in sisal and abaca). The main signals from carbohydrates in the HSQC spectra of the GL fractions corresponded to xylans $\mathbf{X_1}$, $\mathbf{X_2}$, $\mathbf{X_3}$, $\mathbf{X_4}$, $\mathbf{X_5}$, and 4-*O*-methyl-α-D-glucuronic acid ($\mathbf{U_1}$, $\mathbf{U_4}$), despite that GL fractions are known to be enriched in

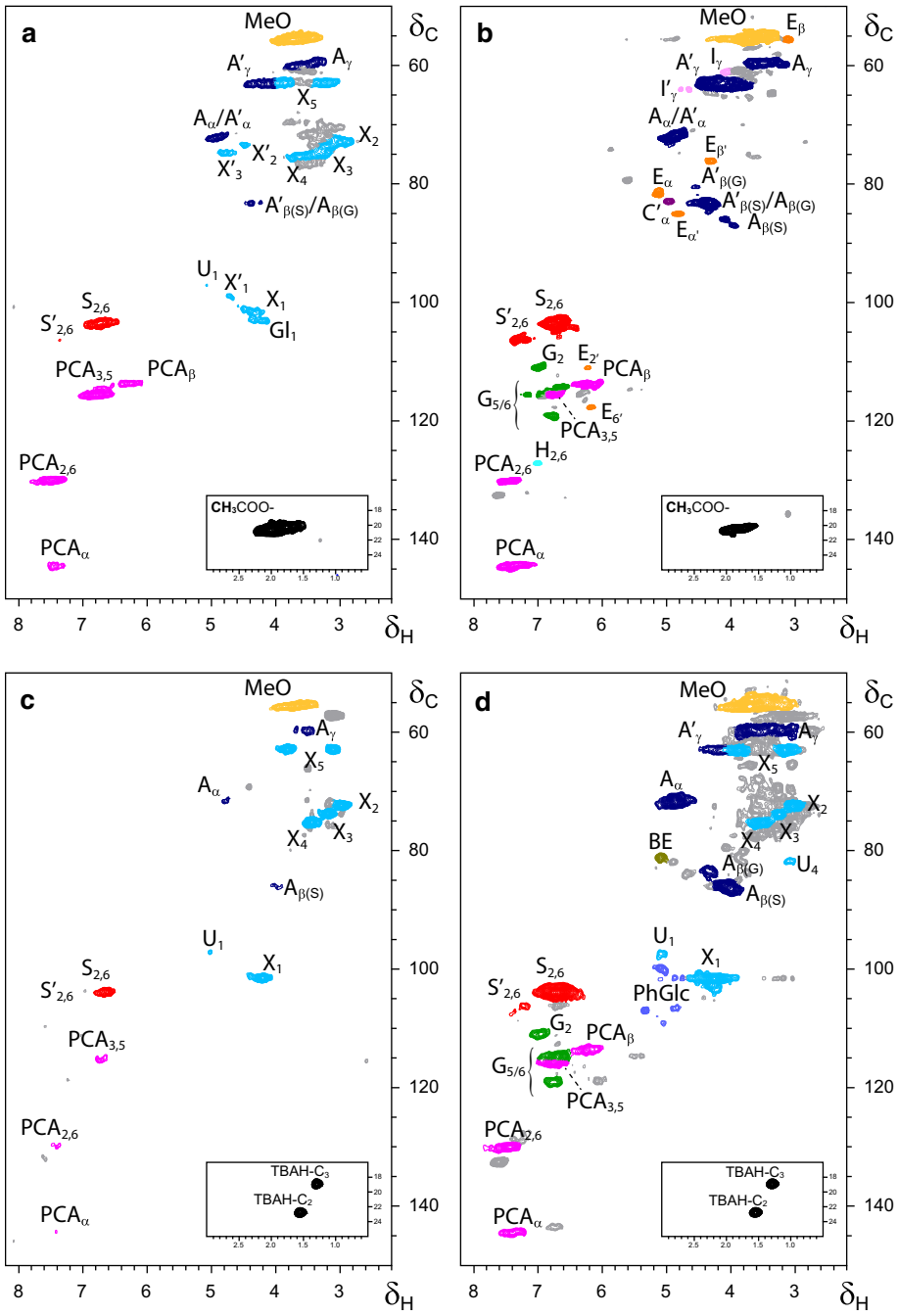

Fig. 3 2D HSQC NMR spectra (δ_C/δ_H 50–150/2.0–8.2) of **a** whole cell walls from abaca, **b** MWL isolated from abaca, **c** GL fraction from abaca, and **d** XL fraction from abaca. See Table 2 for signal assignments and Fig. 4 for the main lignin structures identified

glucans (mostly cellulose), whereas xylan represents only a minor part (9.0 and 4.1 % of total sugars in sisal and abaca, according to Table 1). However, it is important to note that crystalline cellulose is practically "invisible" in the HSQC spectra of the whole cell walls due to its reduced mobility. Therefore, cross-signals from hemicelluloses, and particularly those from xylans, were predominant in the NMR spectra of the GL fractions. To make the cellulose visible in the NMR spectra, the GL and XL fractions were acetylated in DMSO/*N*-methylimidazole/acetic anhydride, as published in Mansfield et al. (2012), and the HSQC spectra were recorded again (Fig. 5). Signals from cellulose were now clearly visible in the spectra of the acetylated samples and easily distinguishable from the signals from xylans. The HSQC spectra of the acetylated GL fractions revealed the presence of strong signals from cellulose and essentially no signals from xylans, corroborating that cellulose is the main carbohydrate present in the GL fractions of both plants, whereas only signals from xylans (and no signals from cellulose) were observed in the spectra of the acetylated XL fractions. In addition, and despite the low intensities of the lignin signals appearing in

Table 2 Assignments of the $^{13}C/^{1}H$ correlation signals observed in the 2D HSQC spectra of whole cell walls, MWLs, and the GL and XL fractions isolated from sisal and abaca

Label	δ_C/δ_H (ppm)	Assignment
Lignin cross-signals		
C_β	53.6/3.07	C_β/H_β in β–β′ resinol substructures (**C**)
MeO	55.6/3.73	C/H in methoxyls (**MeO**)
A_γ	59.4/3.40 and 3.72	C_γ/H_γ in γ-hydroxylated β-*O*-4′ substructures (**A**)
E_β	59.7/2.76	C_β/H_β in spirodienone substructures (**E**)
I_γ	61.3/4.09	C_γ/H_γ in cinnamyl alcohol end groups (**I**)
A'_γ	62.7/3.83–4.30	C_γ/H_γ in γ-acylated β-*O*-4′ substructures (**A′**)
I'_γ	64.0/4.65 and 4.79	C_γ/H_γ in γ-acylated cinnamyl alcohol end groups (**I′**)
C_γ	71.0/3.83 and 4.19	C_γ/H_γ in β–β′ resinol substructures (**C**)
A_α/A'_α	71.8/4.87	C_α/H_α in β-*O*-4′ substructures (**A**, **A′**)
$E_{\beta'}$	79.5/4.11	$C_{\beta'}/H_{\beta'}$ in spirodienone substructures (**E**)
$A'_{\beta(G)}$	80.8/4.58	C_β/H_β in γ-acylated β-*O*-4′ substructures linked to a G unit (**A′**)
E_α	81.2/5.10	C_α/H_α in spirodienone substructures (**E**)
C'_α	82.8/5.00	C_α/H_α in γ-acylated β–β′ tetrahydrofuran structures (**C′**)
$A'_{\beta(S)}$	83.0/4.33	C_β/H_β in γ-acylated β-*O*-4′ substructures linked to a S unit (**A′**)
$A_{\beta(G)}$	83.6/4.29	C_β/H_β in β-*O*-4′ substructures linked to a G unit (**A**)
C_α	84.8/4.67	C_α/H_α in β–β′ resinol substructures (**C**)
$E_{\alpha'}$	84.9/4.88	$C_{\alpha'}/H_{\alpha'}$ in spirodienone substructures (**E**)
$A_{\beta(S)}$	85.9/4.12	C_β/H_β in β-*O*-4′ substructures linked to a S unit (**A**)
B_α	86.9/5.47	C_α/H_α in phenylcoumaran substructures (**B**)
$S_{2,6}$	103.8/6.69	C_2/H_2 and C_6/H_6 in etherified syringyl units (**S**)
$S'_{2,6}$	106.1/7.32 and 106.4/7.19	C_2/H_2 and C_6/H_6 in α-oxidized syringyl units (**S′**)
$E_{2'}$	110.9/6.21	$C_{2'}/H_{2'}$ in spirodienone substructures (**E**)
G_2	110.9/7.00	C_2/H_2 in guaiacyl units (**G**)
PCA_β	113.5/6.27	C_β/H_β in *p*-coumarate (**PCA**)
G_5/G_6	114.9/6.72 and 6.94 118.7/6.77	C_5/H_5 and C_6/H_6 in guaiacyl units (**G**)
$PCA_{3,5}$	115.5/6.77	C_3/H_3 and C_5/H_5 in *p*-coumarate (**PCA**)
$E_{6'}$	117.6/6.17	$C_{6'}/H_{6'}$ in spirodienone substructures (**E**)
$H_{2,6}$	128.0/7.23	C_2/H_2 and C_6/H_6 in *p*-hydroxyphenyl units (**H**)
$PCA_{2,6}$	130.0/7.46	C_2/H_2 and C_6/H_6 in *p*-coumarate (**PCA**)
PCA_α	144.4/7.41	C_α/H_α in *p*-coumarate (**PCA**)
Polysaccharide cross-signals		
X_5	63.2/3.26 and 3.95	C_5/H_5 in β-D-xylopyranoside
X_2	72.9/3.14	C_2/H_2 in β-D-xylopyranoside
X'_2	73.5/4.61	C_2/H_2 in 2-*O*-acetyl-β-D-xylopyranoside
X_3	74.1/3.32	C_3/H_3 in β-D-xylopyranoside
X'_3	74.9/4.91	C_3/H_3 in 3-*O*-acetyl-β-D-xylopyranoside
X_4	75.6/3.63	C_4/H_4 in β-D-xylopyranoside
U_4	81.6/3.08	C_4/H_4 in 4-*O*-methyl-α-D-glucuronic acid
U_1	97.0/5.04	C_1/H_1 in 4-*O*-methyl-α-D-glucuronic acid
X'_1	98.9/4.68	C_1/H_1 in 2-*O*-acetyl-β-D-xylopyranoside
X_1	101.5/4.26	C_1/H_1 in β-D-xylopyranoside
Gl_1	102.9/4.26	C_1/H_1 in β-D-glucopyranoside

the spectra of the unacetylated GL fractions, it was also possible to get information on the structure of the lignin moiety. Signals from the C_α/H_α, C_β/H_β and C_γ/H_γ correlations of β-*O*-4′ substructures (**A**) were the most prominent in the spectra, although they were observed only at low intensities in the HSQC of the abaca-GL fraction, corresponding to its lower Klason lignin content. Minor amounts of phenylcoumarans (**B**) and resinols (**C**) could

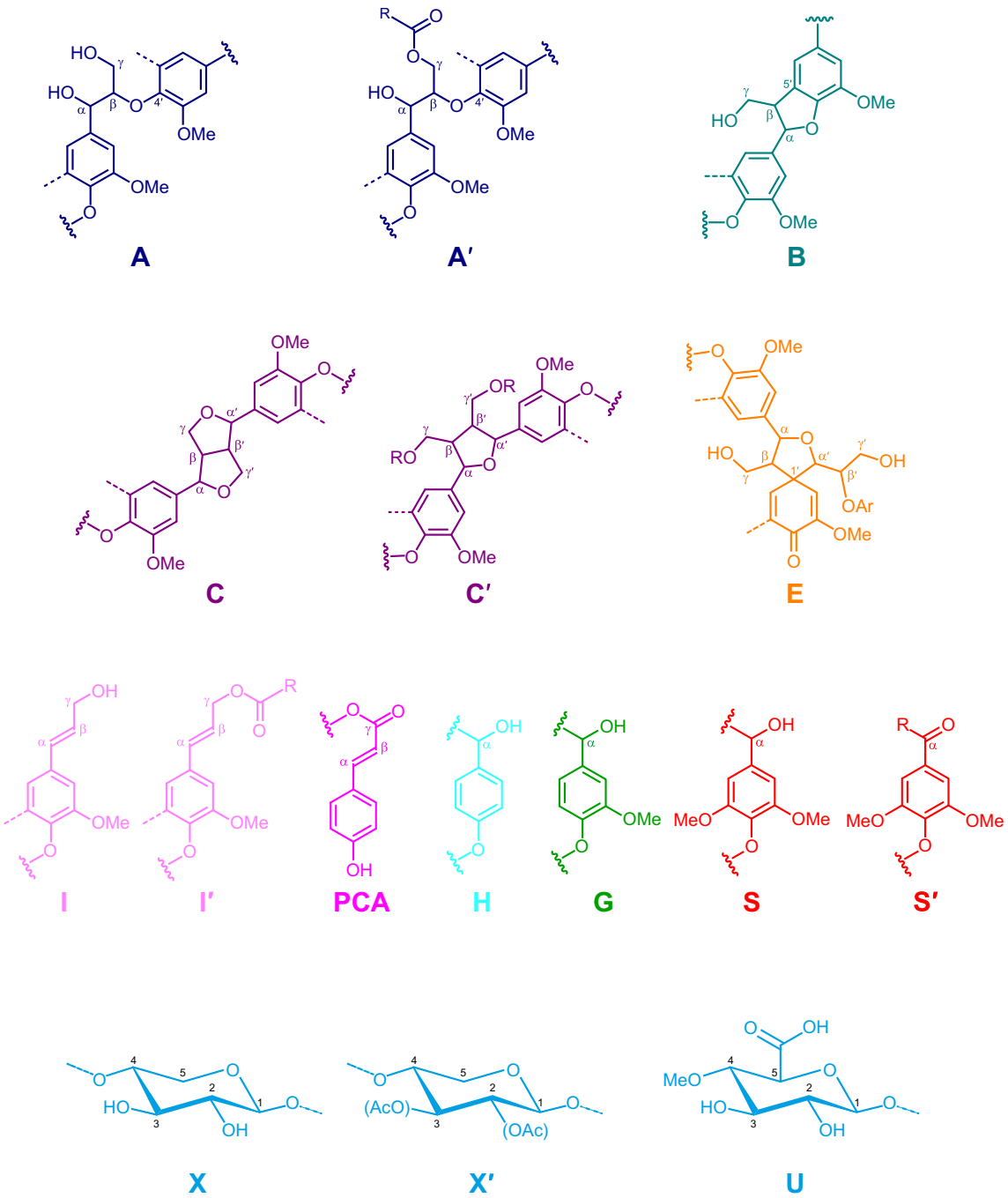

Fig. 4 Main lignin and carbohydrate structures present in the sisal and abaca fractions as identified in the NMR spectra of Figs. 2 and 3. β-*O*-4′-structures (**A**); β-*O*-4′-structures with acylated (by acetates or *p*-coumarates) γ-OH (**A′**); phenylcoumaran structures (**B**); resinol structures (**C**); tetrahydrofuran structure formed by β–β′-coupling of sinapyl alcohol acylated at the γ-carbon (**C′**); spirodienone structures (**E**); *p*-hydroxycinnamyl alcohol end groups (**I**); *p*-hydroxycinnamyl alcohol end groups acylated at the γ-OH (**I′**); *p*-coumarates (**PCA**); *p*-hydroxyphenyl units (**H**); guaiacyl units (**G**); syringyl units (**S**); oxidized syringyl units bearing a carbonyl group at Cα (**S′**); xylopyranose units (**X**); C-2 and/or C-3-acetylated xylopyranose units (**X′**); 4-*O*-methylglucuronic acid units (**U**). The structures are colored to match the assigned contours in the NMR spectra in Figs. 2 and 3

also be detected in the sisal-GL fraction, but could not be observed in abaca-GL fraction. Signals for G- and S-lignin units (and also from *p*-coumarates in the case of abaca) were also observed at low intensities.

The spectra of the XL fractions also presented signals from carbohydrates and lignin, although the signals from lignin are more prominent than in the GL fractions due to their higher Klason lignin content (24.1 and 29.4 % for

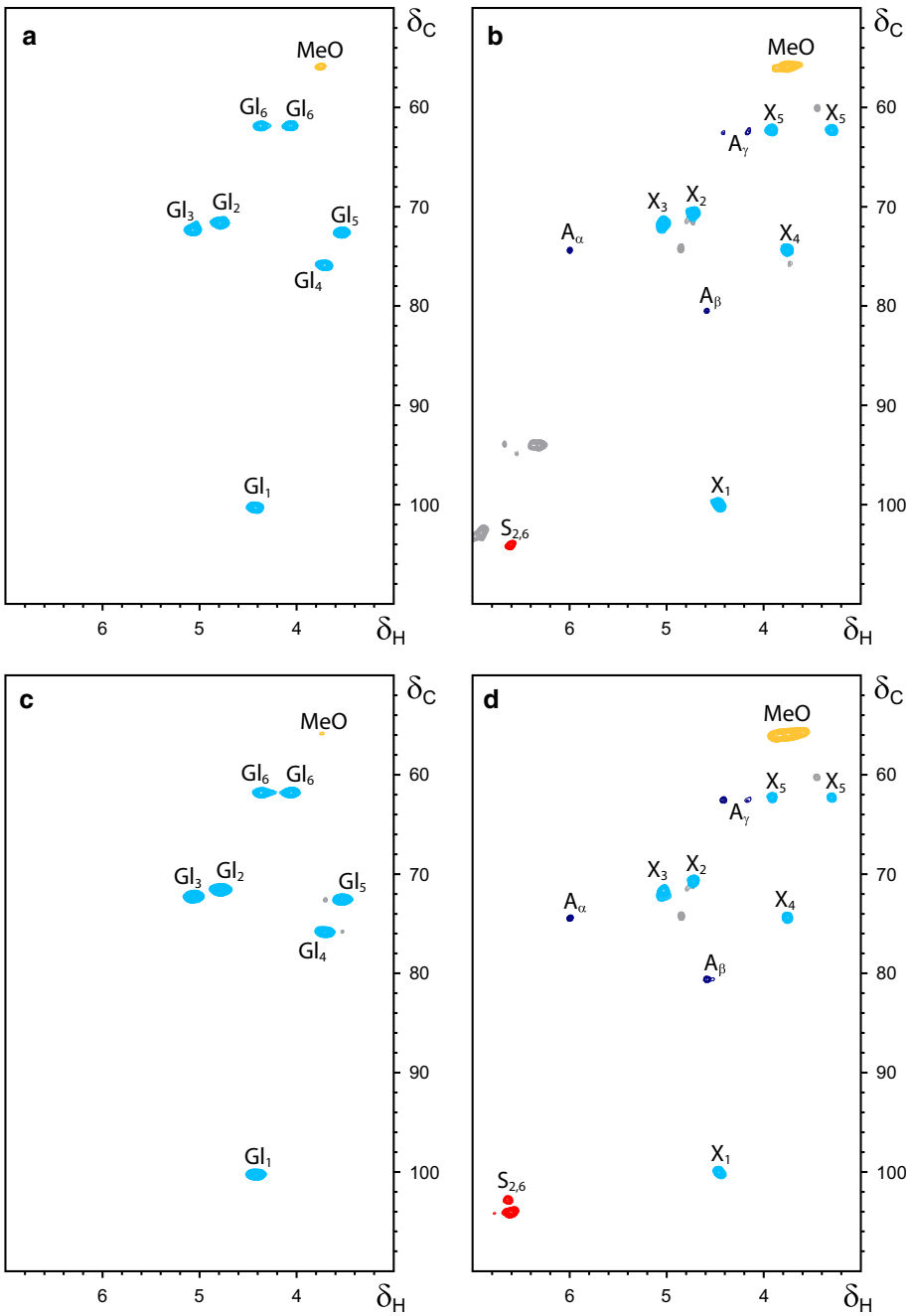

Fig. 5 2D HSQC NMR spectra (δ_C/δ_H 50–110/3.0–7.0) of the acetylated GL and XL fractions. **a** GL fraction from sisal, **b** XL fraction from sisal, **c** GL fraction from abaca, and **d** XL fraction from abaca

sisal-XL and abaca-XL, respectively). Signals from xylans (**X_2**, **X_3**, **X_4**, **X_5**) and the anomeric **X_1** were present in significant amounts as corresponding to the enrichment in xylans in the XL fractions (89.4 and 75.5 % of xylose in sisal and abaca). The HSQC spectra of the acetylated XL fractions (Fig. 5) also corroborate the predominance of xylans, as well as the absence of cellulose, in the XL fractions isolated from sisal and abaca. The most predominant lignin signals in the spectra of the unacetylated XL fractions corresponded to the C_α/H_α, C_β/H_β and C_γ/H_γ correlations of β-*O*-4′ substructures. Signals from G- and S-lignin units were also observed in the spectra of XL fractions, and signals from *p*-coumarates were also present in the spectrum of abaca-XL.

The lignin structural characteristics (abundance of main inter-unit linkages per 100 aromatic units, percentage of γ-acylation, S/G ratio, and *p*-coumarate content) of the GL and XL fractions isolated from sisal and abaca (as determined from integration of $^{13}C/^{1}H$ correlation signals in the HSQC spectra) are shown in Table 3, together with those of their respective whole cell walls and MWLs, for comparison. The data indicates that, in both plants, the XL

Table 3 Structural characteristics (abundance of main inter-units linkages, percentage of γ-acylation, S/G ratio, and *p*-coumarate content) of the GL and XL fractions isolated from sisal and abaca, and in their respective whole cell walls (CW) and MWLs for comparison, as determined from integration of ^{13}C–^{1}H correlation signals in the HSQC spectra

	Sisal				Abaca			
	CW	MWL	GL	XL	CW	MWL	GL	XL
Lignin inter-unit linkages (per 100 aromatic units)								
β-*O*-4′ aryl ethers (**A**)	80	80	52	78	79	80	40	78
Phenylcoumarans (**B**)	0	3	4	0	0	1	0	1
Resinols (**C**)	3	3	3	2	0	0	0	0
Spirodienones (**D**)	0	4	0	0	0	1	0	0
γ-Acylation (%)	60	65	0	0	75	80	0	4
S/G ratio	3.3	3.5	3.0[a]	6.5	7.5	7.5	5.0[a]	12.0
p-Coumarates[b]	0	0	0	0	65	45	12	10

[a] Might be overestimated due to the low amounts of lignin units, particularly G units

[b] Molar content as percentage of total lignin units (H + G + S = 100)

fractions are enriched in S-lignin units (S/G ratios of 6.5 and 12.0 in sisal-XL and abaca-XL), whereas GL fractions have comparatively more G units and thus lower S/G ratios (3.0 and 5.0 in sisal-GL and abaca-GL). The differences in lignin composition are also reflected in the abundances of side chain inter-unit linkages, and thus XL fractions are enriched in β-*O*-4′ alkyl-aryl ether linkages (78 linkages per 100 aromatic units in sisal and abaca), whereas GL fractions have less β-*O*-4′ alkyl-aryl ether linkages (only 52 and 40 linkages per 100 aromatic units in sisal and abaca) and more condensed side chain linkages, particularly more β-5′ phenylcoumarans, corresponding to a lignin with more G units. Similar results were also found in the LCC fractions isolated from eucalyptus wood (Li et al. 2011) that consisted of a xylan-enriched fraction with a predominance of S-lignin units and a glucan-enriched fraction with more G-lignin units. This fact suggests that the lignin moieties present in the different LCC fractions isolated from sisal and abaca are structurally different from each other and indicates the presence of two types of lignins: a lignin that is enriched in S units, less condensed, and that is preferentially associated with xylans; and a lignin with more G units, more condensed, and that is preferentially associated with glucans. Several other studies have revealed the inhomogeneities in lignin composition and structure in plant cell walls, including hardwoods, softwoods, and herbaceous plants (Önnerud and Gellerstedt 2003a, b; Sun et al. 2003, 2013; Wen et al. 2015). These studies have indicated that there are significant differences in the chemical structure of the lignins depending on their histological origin and concluded that the lignins from secondary cell walls are rich in S-lignin units and present higher amounts of ether linkages, whereas the lignins in the middle lamella are enriched in G-lignin units and present more condensed lignin inter-unit linkages.

On the other hand, the 2D-NMR spectra also revealed additional features of the isolated LCC fractions. The spectra of the GL and XL fractions showed the presence of four strong and well-resolved signals at δ_C/δ_H 13.19/0.92, 18.92/1.29, 22.77/1.55, and 57.29/3.1, which were not present in the spectra of the whole cell walls and MWLs and that corresponded to the C-4, C-3, C-2, and C-1 of TBAH (only the signals from C-3 and C-2 of TBAH are shown in the insets of Figs. 2, 3). The presence of these signals indicates the occurrence of significant amounts of TBAH remnants in the GL and XL fractions, despite their extensive washing during the isolation process. This finding implies that the yields of the isolated LCC fractions might be overestimated, which will preclude a good mass balance calculation.

Structural modifications (deacetylation) of hemicelluloses and lignin during the LCC fractionation process

The HSQC spectra also revealed that some structural modifications of the carbohydrates and lignin polymers in the LCC fractions have occurred during fractionation. Hence, signals from acetylated xylans ($\mathbf{X'_1}$, $\mathbf{X'_2}$, and $\mathbf{X'_3}$), that were present in important amounts in the spectra of the whole cell walls of sisal and abaca completely disappeared from the spectra of the GL and XL fractions, suggesting that the acetate groups attached to hemicelluloses were hydrolyzed and removed during the LCC fractionation process. Likewise, the signals at δ_C/δ_H 62.7/3.83–4.30 corresponding to the C_γ/H_γ correlations of γ-acylated β-*O*-4′ substructures (**A′**) also disappeared from the HSQC spectra of GL and XL fractions. Moreover, the strong signal at δ_C/δ_H 83.0/4.33 corresponding to the C_β/H_β correlations of γ-acylated β-*O*-4′ substructures linked to an S unit ($A'_{\beta(S)}$) disappeared and shifted to δ_C/δ_H 85.9/4.12 for normal (γ-OH) β-*O*-4′ substructures linked to an S unit,

indicating that the groups acylating the γ-OH of the lignin side chain have also been largely hydrolyzed and removed during the LCC isolation process. In the case of sisal, the signal at δ_C/δ_H 80.8/4.58, assigned to γ-acylated β-*O*-4′ substructures linked to G units, also disappeared, confirming the removal of the groups acylating the γ-OH of the lignin side chain. Only minor amounts of the signal for the C_γ/H_γ correlations of γ-acylated β-*O*-4′ substructures (A'_γ) could be observed in the spectrum of XL fraction from abaca (that was estimated to account for around 4 % lignin acylation). On the other hand, the characteristic signals from acetate groups (attached to hemicelluloses and/or lignin) that are clearly visible in the HSQC spectra of the whole cell walls and the isolated MWLs around δ_C/δ_H 20–21/1.50–2.00 (see inset in the HSQC spectra of Figs. 2, 3) also completely disappeared from the spectra of the GL and XL fractions, corroborating that acetates attached to the hemicelluloses and lignin have been completely removed during the LCC isolation process. In the case of abaca, the spectrum of GL and particularly the spectrum of the XL fraction indicated the occurrence of minor amounts of *p*-coumarates. Since only a minor degree of acylation of the γ-OH was observed in the spectrum of XL fraction from abaca (4 % acylation), it is possible to conclude that most of the *p*-coumarates have also been hydrolyzed and only a minor part of them still remain attached to the lignin. The structural modifications observed in the carbohydrates and lignin—hydrolysis and removal of acetates from hemicelluloses and the acyl groups attached to the lignin—may have been most probably due to the use of TBAH, a strong base that may alter the structure of these polymers during the fractionation process. Likewise, it can be envisaged that other groups (i.e., *p*-hydroxybenzoates) that are also acylating the γ-carbon of the lignin in other plants (Rencoret et al. 2013; Lu et al. 2015) may behave similarly and suffer from hydrolysis during the LCC fractionation.

The eventual hydrolysis of acetates attached to the γ-OH of the lignin side chains during the LCC fractionation process was also monitored using a modification of the DFRC method by substituting acetylating reagents with propionylating ones (DFRC′), as previously published (Ralph and Lu 1998; del Río et al. 2007). The chromatograms of the DFRC′ degradation products of the GL and XL fractions are shown in Fig. 6. The chromatograms of the DFRC′ degradation products of the corresponding MWLs are also shown for comparison. The relative abundances of the γ-OH and γ-acetylated lignin units (G, G_{ac}, S and S_{ac}), as well as the percentages of acetylated G and S units (%G_{ac}, %S_{ac}), in the GL and XL fractions isolated from sisal and abaca, and in their respective MWLs, are shown in Table 4. The MWLs from sisal and abaca released the *cis* and *trans* isomers of guaiacyl (*c*-G and *t*-G) and syringyl (*c*-S and *t*-S) lignin monomers (as their propionylated derivatives) arising from normal (γ-OH) units in lignin. In addition, the presence of γ-acetylated guaiacyl (*c*-G_{ac} and *t*-G_{ac}) and syringyl (*c*-S_{ac} and *t*-S_{ac}) lignin units (as their phenol-propionylated derivatives) could also be clearly observed in the chromatograms. The high extent of γ-acetylation of sisal MWL included both S units (78 % of all S units are acetylated) and G units (46 % of all G units are acetylated), whereas in the case of abaca MWL γ-acetylation occurred predominantly on S units (83 % of all S units are acetylated) and only a minor degree of acetylation was observed on G units (5 % of all G units are acetylated), in agreement with previous studies (del Río et al. 2007, 2008). However, and as expected, the GL and XL fractions only released the *cis* and *trans* isomers of guaiacyl (*c*-G and *t*-G) and syringyl (*c*-S and *t*-S) lignin monomers arising from normal (γ-OH) units in lignin, whereas the γ-acetylated guaiacyl (*c*-G_{ac} and *t*-G_{ac}) and syringyl (*c*-S_{ac} and *t*-S_{ac}) lignin units were completely absent in the chromatograms. This indicates that the acetate groups acylating the γ-OH of the lignin side chain have been completely hydrolyzed during the LCC fractionation process, as already observed by 2D-NMR.

Lignin–carbohydrate linkages in the isolated LCC fractions

We also investigated the occurrence of lignin–carbohydrate linkages in the LCC fractions isolated from sisal and abaca. It is generally accepted that different types of linkages occur between lignin and carbohydrates in plant cell walls, including phenyl glycosides (PhGlc), esters to the lignin γ-OH (Est), and benzyl ether linkages (BE) (Fig. 7). Phenyl glycoside linkages (PhGlc) give a group of characteristic signals for the anomeric carbon at around δ_C/δ_H 99–104/4.8–5.2 (Terashima et al. 1996; Balakshin et al. 2007, 2011; Miyagawa et al. 2014). Phenyl glycoside linkages have been detected by NMR in other lignin–carbohydrate preparations from several woods, including loblolly pine, white birch, poplar, and spruce (Balakshin et al. 2011; Yuan et al. 2011; Du et al. 2014). Signals for phenyl glycoside linkages, however, could only be detected in the spectrum of XL from abaca, and to a minor extent in the spectrum of XL from sisal. These signals would most probably correspond to phenyl glycoside linkages between G- and S-lignin units to xylose units in xylans. No phenyl glycoside linkages, however, were detected in the GL fractions from sisal and abaca, which could be due either to their very low concentration (as lignin content is very low, ~4–8 %) or to the absence of direct phenyl glycoside linkages between cellulose and lignin. On the other hand, signals for carbohydrates ester linked to the lignin (Est), usually occurring between the γ-OH of the lignin side chain and the carboxylic group of the uronic acid (Li and

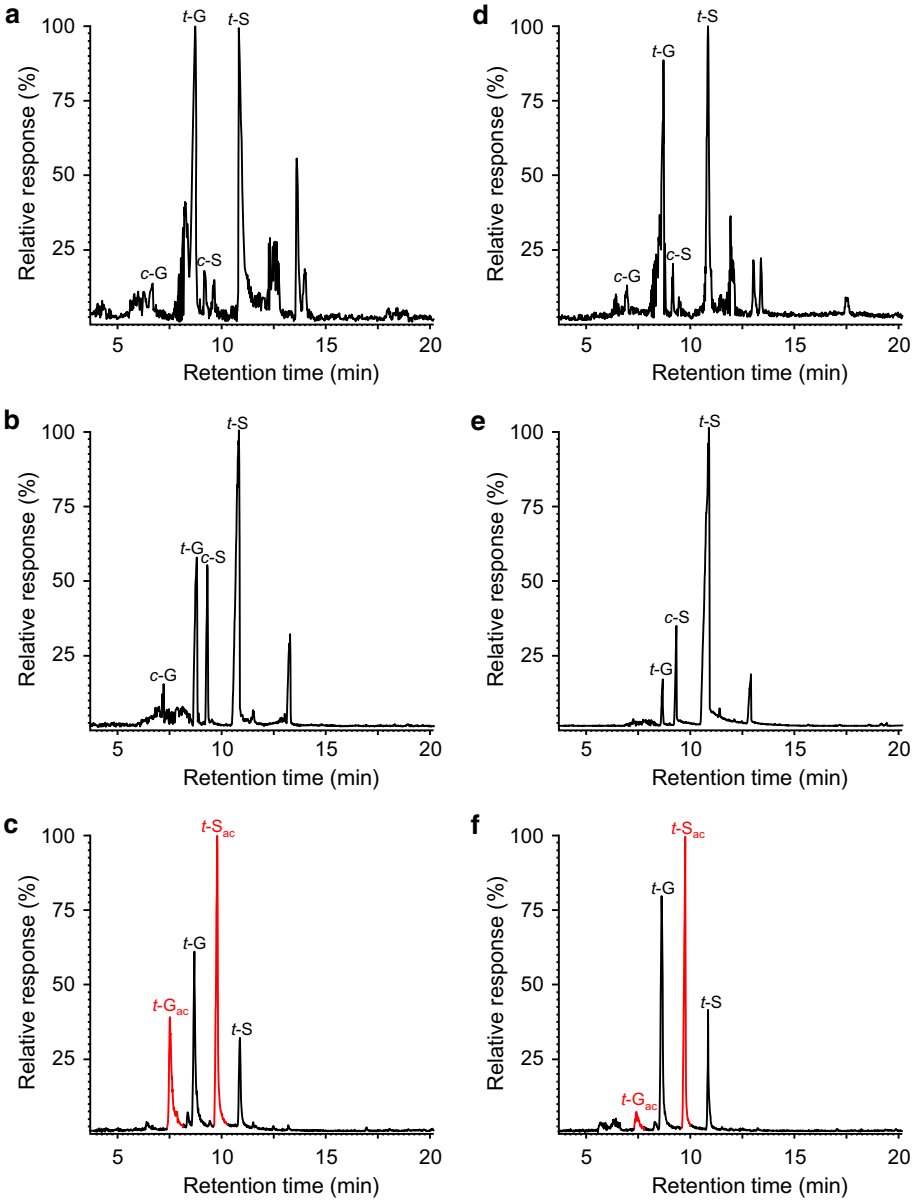

Fig. 6 Reconstructed ion chromatograms (*m/z* 222 + 236 + 252 + 266) of the DFRC′ degradation products of: **a** GL fraction from sisal, **b** XL fraction from sisal, and **c** MWL isolated from sisal, and **d** GL fraction from abaca, **e** XL fraction from abaca, and **f** MWL isolated from abaca. *c*-G, *t*-G, *c*-S, and *t*-S are the *cis*- and *trans*-guaiacyl and syringyl monomers, respectively. *c*-G_{ac}, *t*-G_{ac}, *c*-S_{ac}, and *t*-S_{ac} are the originally γ-acetylated *cis*- and *trans*-guaiacyl and syringyl monomers, respectively

Table 4 Relative abundance of γ-OH and γ-acetylated lignin units (G, G_{ac}, S, and S_{ac}), percentage of acetylated G and S units and S/G ratios, in the GL and XL fractions isolated from sisal and abaca, and in their respective MWLs for comparison, as determined on DFRC′

	Sisal			Abaca		
	MWL	GL	XL	MWL	GL	XL
G_{ac}	17	0	0	2	0	0
G	20	50	25	40	46	19
% acetylated G units	46	0	0	5	0	0
S_{ac}	49	0	0	48	0	0
S	14	50	75	10	54	81
% acetylated S units	78	0	0	83	0	0

Helm 1995), should appear around δ_C/δ_H 65–62/4.0–4.5 in the HSQC spectra (Balakshin et al. 2007, 2011). However, this signal is particularly difficult to observe when the lignin is extensively acylated at the γ-OH, as in sisal and abaca, since it would overlap with the strong signal at δ_C/δ_H 62.7/3.83–4.30 from γ-acylated β-*O*-4′ substructures (**A′**). Signals for ester linkages to the lignin γ-OH (Est) could not be observed in the HSQC spectra of the XL fractions, but if originally present they might have also been hydrolyzed during the LCC isolation process, as also occurred with other groups (acetates and *p*-coumarates) acylating the lignin γ-OH. The occurrence of uronic γ-ester linkages in the LCC fractions may therefore be biased

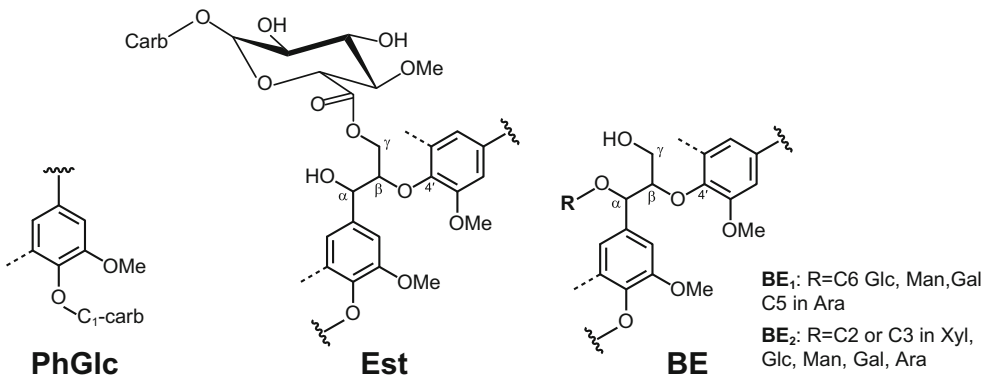

Fig. 7 Main lignin–carbohydrate linkages observed in plants: phenyl glycosides (**PhGlc**), lignin γ-esters (**γ-Est**), and benzyl ethers (**BE**)

using the present LCC isolation protocol. Finally, and regarding benzyl ether lignin–carbohydrate linkages (BE), two types of linkages have been reported to occur: linkages between the α-position of a lignin unit and the primary OH groups of carbohydrates (BE_1, at C-6 of glucose, galactose, and mannose and C-5 of arabinose) giving a characteristic signal around δ_C/δ_H 80–81/4.5–4.7, and linkages between the α-position of a lignin unit and secondary OH groups of carbohydrates (BE_2), mainly of xylan type, giving a characteristic signal around δ_C/δ_H 80–81/4.9–5.1 (Toikka et al. 1998; Toikka and Brunow 1999; Tokimatsu et al. 1996; Balakshin et al. 2011). Signals for BE_1 linkages were observed in LCC fractions isolated from several hardwoods and softwoods, including loblolly pine, white birch, poplar, and spruce (Balakshin et al. 2011; Yuan et al. 2011; Du et al. 2014), although they could not be detected in the GL and XL fractions isolated from sisal and abaca. In the XL fractions isolated from sisal and abaca, only the signal at δ_C/δ_H 81.0/5.08 for BE_2-type linkages was observed, corresponding to an LCC fraction enriched in xylans and lignin, and which according to the literature would correspond to the Cα-position of lignin–xylan benzyl ether linkages (Toikka et al. 1998; Toikka and Brunow 1999; Tokimatsu et al. 1996; Balakshin et al. 2011). Although this signal might partially overlap with the signal for the C_α/H_α correlation of spirodienones, the absence in the XL fractions of the respective signals for the $C_{\alpha'}/H_{\alpha'}$ and $C_{\beta'}/H_{\beta'}$ correlations of spirodienones supports the occurrence of lignin–xylan linkages in this fraction. In contrast, no signals for BE lignin–carbohydrate linkages could be detected in the GL fractions, corresponding to a fraction depleted in both lignin and xylans.

Conclusions

The LCC fractionation protocol recently developed for hardwoods and softwoods (Li et al. 2011; Du et al. 2013) has now been extended to herbaceous plants (sisal and abaca) and has proven to be a useful tool to get additional insights into the structure of LCCs, confirming the truly "universal" application of the protocol to any type of lignocellulosic plant material. Two different LCC fractions, namely a glucan–lignin (GL) and a xylan–lignin (XL) fraction, were isolated from sisal and abaca. However, and despite extensive washing, significant amounts of TBAH remained in the isolated fractions affecting the yield and hindering the assessment of a precise mass balance. The GL fractions were enriched in glucans and depleted in lignin, while the XL fractions were depleted in glucans and enriched in xylans and lignin. The structural characteristics of the lignins in the GL and XL fractions were studied by 2D NMR and by a modification of the DFRC method and indicated that XL fractions are enriched in S-lignin units and β-*O*-4′ alkyl-aryl ether linkages, whereas GL fractions have more G-lignin units and less β-*O*-4′ alkyl-aryl ethers per lignin unit, suggesting that the lignin polymer is not homogeneous within the same plant and that different lignins with different compositions and structures might be present. In addition, several chemical linkages (phenylglycosides and benzyl ethers) have been observed to occur between lignin and xylans in these plants. Finally, it has also been proven that this fractionation protocol has also some limitations, as it affects the structure of the carbohydrates and the lignin polymer. The analyses indicated that the acetate groups that are attached to the carbohydrates and the acetates and *p*-coumarates attached to the lignins in sisal and abaca were completely hydrolyzed and removed during the LCC fractionation. Likewise, it can be envisaged that other groups (*p*-hydroxybenzoates) that are also acylating the γ-carbon of the lignin in other plants may behave similarly and suffer from hydrolysis during the LCC fractionation. Similarly, the occurrence of γ-ester linkages between carbohydrates and lignin would also be biased by using this fractionation approach. Consequently, it seems that the isolated fractions would mostly reflect alkali-stable LCC fractions that might be somehow different from the real LCC network. Therefore, it is apparent

that this fractionation protocol might cause ester hydrolysis and that it must be applied with caution when used for detailed structural characterization of the cell wall components, in particular in the case of plants with acetylated hemicelluloses or having lignins with a high extent of acylation.

Author contribution statement J.C.R. conceived and designed the research; P.P., E.M.C., and J.R. conducted the experiments; J.C.R., J.R., A.G., and A.T.M. analyzed the data; J.C.R. and J.R. wrote the manuscript. All authors read and approved the manuscript.

Acknowledgments This study has been funded by the Spanish Projects AGL2011-25379, AGL2014-53730-R and CTQ2014-60764-JIN (co-financed by FEDER funds); the CSIC project 2014-40E-097; and the EU-Projects LIGNODECO (KBBE-2009-3-244362); and INDOX (KBBE-2013-7-613549). Analysis of carbohydrates was performed by Carlos Vila (Celbiotech Research Group, Polytechnic University of Catalonia, Tarrasa, Spain). We finally thank Dr. Manuel Angulo for performing the NMR analyses that were acquired in a Bruker Advance III 500 MHz instrument from the NMR facilities of the General Research Services of the University of Seville (SGI-CITIUS).

References

Balakshin MY, Capanema EA, Chang HM (2007) A fraction of MWL with a high concentration of lignin–carbohydrate linkages: isolation and 2D NMR spectroscopic analysis. Holzforschung 61:1–7

Balakshin M, Capanema E, Gracz H, Chang HM, Jameel H (2011) Quantification of lignin–carbohydrate linkages with high-resolution NMR spectroscopy. Planta 233:1097–1110

Björkman A (1956) Studies on finely divided wood. Part I. Extraction of lignin with neutral solvents. Svensk Papperstidn 59:477–485

Cadena EM, Du X, Gellerstedt G, Li J, Fillat A, García-Ubasart J, Vidal T, Colom JF (2011) On hexenuronic acid (HexA) removal and mediator coupling to pulp fiber in the laccase/mediator treatment. Bioresour Technol 102:3911–3917

Darwill A, McNeil M, Albersheim P, Delmer D (1980) The primary cell-walls of flowering plants. In: Tolbert N (ed) The biochemistry of plants. Academic Press, New York, pp 91–162

del Río JC, Gutiérrez A, Martínez AT (2004) Identifying acetylated lignin units in non-wood fibers using pyrolysis-gas chromatography/mass spectrometry. Rapid Commun Mass Spectrom 18:1181–1185

del Río JC, Marques G, Rencoret J, Martínez AT, Gutiérrez A (2007) Occurrence of naturally acetylated lignin units. J Agric Food Chem 55:5461–5468

del Río JC, Rencoret J, Marques G, Gutiérrez A, Ibarra D, Santos JI, Jiménez-Barbero J, Zhang L, Martínez AT (2008) Highly acylated (acetylated and/or *p*-coumaroylated) native lignins from diverse herbaceous plants. J Agric Food Chem 56:9525–9534

del Río JC, Rencoret J, Prinsen P, Martínez AT, Ralph J, Gutiérrez A (2012a) Structural characterization of wheat straw lignin as revealed by analytical pyrolysis, 2D-NMR, and reductive cleavage methods. J Agric Food Chem 60:5922–5935

del Río JC, Prinsen P, Rencoret J, Nieto L, Jiménez-Barbero J, Ralph J, Martínez AT, Gutiérrez A (2012b) Structural characterization of the lignin in the cortex and pith of elephant grass (*Pennisetum purpureum*) stems. J Agric Food Chem 60:3619–3634

del Río JC, Lino AG, Colodette JL, Lima CF, Gutiérrez A, Martínez AT, Lu F, Ralph J, Rencoret J (2015) Differences in the chemical structures of the lignins from sugarcane bagasse and straw. Biomass Bioenergy 81:322–338

Du X, Gellerstedt G, Li J (2013) Universal fractionation of lignin–carbohydrate complexes (LCCs) from lignocellulosic biomass: an example using spruce wood. Plant J 74:328–338

Du X, Pérez-Boada M, Fernández C, Rencoret J, del Río JC, Jiménez-Barbero J, Li J, Gutiérrez A, Martínez AT (2014) Analysis of lignin–carbohydrate and lignin–lignin linkages after hydrolase treatment of xylan–lignin, glucomannan–lignin and glucan–lignin complexes from spruce wood. Planta 239:1079–1090

Fengel D, Wegener G (1984) Wood: chemistry, ultrastructure, reactions. Walter de Gruyter, Berlin

Kim H, Ralph J, Akiyama T (2008) Solution-state 2D NMR of ball-milled plant cell-wall gels in DMSO-d_6. Bioenergy Res 1(1):56–66

Koshijima T, Watanabe T (2003) Association between lignin and carbohydrates in wood and other plant tissues. Springer, Berlin

Landucci LL, Deka GC, Roy DNA (1992) ^{13}C NMR study of milled wood lignins from hybrid *Salix* clones. Holzforschung 46:505–511

Lawoko M, Henriksson G, Gellerstedt G (2003) New method for quantitative preparation of lignin–carbohydrate complex from unbleached softwood kraft pulp: lignin–polysaccharide networks I. Holzforschung 57:69–74

Lawoko M, Henriksson G, Gellerstedt G (2005) Structural differences between the lignin–carbohydrate complexes present in wood and in chemical pulps. Biomacromolecules 6:3467–3473

Li K, Helm RF (1995) Synthesis and rearrangement reactions of ester-linked lignin–carbohydrate model compounds. J Agric Food Chem 43:2098–2103

Li J, Martin-Sampedro R, Pedrazzi C, Gellerstedt G (2011) Fractionation and characterization of lignin–carbohydrate complexes (LCCs) from eucalyptus fibers. Holzforschung 65:43–50

Lu F, Ralph J (1997a) Derivatization followed by reductive cleavage (DFRC method), a new method for lignin analysis: protocol for analysis of DFRC monomers. J Agric Food Chem 45:2590–2592

Lu F, Ralph J (1997b) The DFRC method for lignin analysis. Part 1. A new method for β-aryl ether cleavage: lignin model studies. J Agric Food Chem 45:4655–4660

Lu F, Ralph J (1998) The DFRC method for lignin analysis. 2. Monomers from isolated lignin. J Agric Food Chem 46:547–552

Lu F, Ralph J (1999) Detection and determination of *p*-coumaraloylated units in lignin. J Agric Food Chem 47:1985–1992

Lu F, Ralph J (2005) Novel β–β-structures in lignins incorporating acylated monolignols. In: Proceedings of the Thirteenth International Symposium on Wood, Fiber, and Pulping Chemistry, APPITA, New Zealand, pp 233–237

Lu F, Karlen SD, Regner M, Kim H, Ralph SA, Sun R-C, K-i Kuroda, Augustin MA, Mawson R, Sabarez H, Singh T, Jimenez-Monteon G, Zakaria S, Hill S, Harris PJ, Boerjan W, Wilkerson CG, Mansfield SD, Ralph J (2015) Naturally *p*-hydroxybenzoylated lignins in palms. BioEnergy Res 8:934–952

Mansfield SD, Kim H, Lu F, Ralph J (2012) Whole plant cell wall characterization using solution-state 2D NMR. Nat Protcols 7:1579–1589

Marques G, Gutiérrez A, del Río JC, Evtuguin DV (2010) Acetylated heteroxylan from *Agave sisalana* and its behaviour during alkaline pulping and TCF/ECF bleaching. Carbohydr Polym 81:517–523

Martínez AT, Rencoret J, Marques G, Gutiérrez A, Ibarra D, Jiménez-Barbero J, del Río JC (2008) Monolignol acylation and lignin

structure in some nonwoody plants: a 2D-NMR study. Phytochemistry 69:2831–2843

Miyagawa Y, Mizukami T, Kamitakahara H, Takano T (2014) Synthesis and fundamental HSQC NMR data of monolignol β-glycosides, dihydromonolignol β-glycosides and *p*-hydroxybenzaldehyde derivative β-glycosides for the analysis of phenyl glycoside type lignin–carbohydrate complexes (LCCs). Holzforschung 68:747–760

Önnerud H, Gellerstedt G (2003a) Inhomogeneities in the chemical structure of spruce lignin. Holzforschung 57:165–170

Önnerud H, Gellerstedt G (2003b) Inhomogeneities in the chemical structure of hardwood lignins. Holzforschung 57:255–265

Ralph J (1996) An unusual lignin from kenaf. J Nat Prod 59:341–342

Ralph J (2010) Hydroxycinnamates in lignification. Phytochem Rev 9:65–83

Ralph J, Lu F (1998) The DFRC method for lignin analysis. 6. A simple modification for identifying natural acetates in lignin. J Agric Food Chem 46:4616–4619

Ralph J, Hatfield RD, Quideau S, Helm RF, Grabber JH, Jung H-JG (1994) Pathway of *p*-coumaric acid incorporation into maize lignin as revealed by NMR. J Am Chem Soc 116:9448–9456

Ralph J, Lundquist K, Brunow G, Lu F, Kim H, Schatz PF, Marita JM, Hatfield RD, Ralph SA, Christensen JH et al (2004) Lignins: natural polymers from oxidative coupling of 4-hydroxyphenylpropanoids. Phytochem Rev 3:29–60

Ralph SA, Ralph J, Landucci L (2009) NMR database of lignin and cell wall model compounds. https://www.glbrc.org/databases_and_software/nmrdatabase/. Accessed on July 2015

Rencoret J, Marques G, Gutiérrez A, Nieto L, Santos JI, Jiménez-Barbero J et al (2009) HSQC-NMR analysis of lignin in woody (*Eucalyptus globulus* and *Picea abies*) and non-woody (*Agave sisalana*) ball-milled plant materials at the gel state. Holzforschung 63(6):691–698

Rencoret J, Ralph J, Marques G, Gutiérrez A, Martínez AT, del Río JC (2013) Structural characterization of lignin isolated from coconut (*Cocos nucifera*) coir fibers. J Agric Food Chem 61:2434–2445

Sjöström E (1993) Wood constituents, fundamentals and applications, 2nd edn. Academic Press, New York

Sun J-X, Sun X-F, Sun R-C, Fowler P, Baird MS (2003) Inhomogeneities in the chemical structure of sugarcane bagasse lignin. J Agric Food Chem 51:6719–6725

Sun S-L, Wen J-L, Ma M-G, Li M-F, Sun R-C (2013) Revealing the structural inhomogeneity of lignins from sweet sorghum stem by successive alkali extractions. J Agric Food Chem 61:4226–4235

Tappi Standard Test Methods 2004–2005 (2004) Tappi test methods. Tappi Press, Atlanta

Teleman A, Tenkanen M, Jacobs A, Dahlman O (2002) Characterization of *O*-acetyl-(4-*O*-methylglucurono)xylan isolated from birch and beech. Carbohydr Res 337:373–377

Terashima N, Ralph SA, Landucci LL (1996) New facile syntheses of monolignol glucosides; *p*-glucocoumaryl alcohol, coniferin, and syringin. Holzforschung 50:151–155

Toikka M, Brunow G (1999) Lignin–carbohydrate model compounds. Reactivity of methyl 3-*O*-(α-L-arabinofuranosyl)-β-D-xylopyranoside and methyl β-D-xylopyranoside towards a β-*O*-4-quinone methide. J Chem Soc Perkin Trans 1:1877–1883

Toikka M, Sipilä J, Teleman A, Brunow G (1998) Lignin–carbohydrate model compounds. Formation of lignin–methyl arabinoside and lignin–methyl galactoside benzyl ethers via quinone methide intermediates. J Chem Soc Perkin Trans 1:3813–3818

Tokimatsu T, Umezawa T, Shimada M (1996) Synthesis of four diastereomeric lignin carbohydrate complexes (LCC) model compounds composed of a β-*O*-4 lignin model linked to methyl beta-D-glucoside. Holzforschung 50:156–160

Wen J-L, Sun S-L, Xue B-L, Sun R-C (2015) Structural elucidation of inhomogeneous lignins from bamboo. Int J Biol Macromol 77:250–259

Willför S, Sjöholm R, Laine C, Roslund M, Hemming J, Holmbom B (2003) Characterisation of water-soluble galactoglucomannans from Norway spruce wood and thermomechanical pulp. Carbohydr Polym 52:175–187

Yuan T-Q, Sun S-N, Xu F, Sun R-C (2011) Characterization of lignin structures and lignin–carbohydrate complex (LCC) linkages by quantitative ^{13}C and 2D HSQC NMR spectroscopy. J Agric Food Chem 59:10604–10614